

1 **Metabolomic Alterations in Crimean Congo Hemorrhagic Fever**
2 **Explored Through a Nationwide Study Using NMR Spectroscopy**

3 *Oktay Göcenler^{1,#}, Kerem Kahraman^{1,#}, Derya Yapar^{2,3}, Yaren Kahraman¹, Cengizhan*
4 *Büyükdağ¹, Gülen Esken⁴, Serena Ozabrahamyan⁵, Tayfun Barlas⁴, Yüksel Karadağ³, Aysel*
5 *Kocagül Çelikbaş^{2,3}, Füsun Can^{4,6}, Nurcan Baykam^{2,3}, Mert Kuşkucu^{4,7}, Önder Ergönül^{4,7},*
6 *Çağdaş Dağ^{1, 4,*}*

7 ¹Nanofabrication and Nanocharacterization Center for Scientific and Technological Advanced
8 Research (n²STAR), Koç University, İstanbul, Türkiye

9 ²Hitit University, School of Medicine, Çorum, Türkiye

10 ³Department of Infectious Diseases and Clinical Microbiology, Çorum Erol Olçok Training and
11 Research Hospital, Çorum, Türkiye

12 ⁴Koç University Isbank Center for Infectious Diseases (KUISCID), Koc University, Istanbul,
13 Türkiye

14 ⁵The Ohio State University Wexner Medical Center, Columbus, USA

15 ⁶Koç University School of Medicine, Department of Medical Microbiology, Istanbul, Türkiye

16 ⁷Koç University School of Medicine, Department of Clinical Microbiology and Infectious
17 Diseases, Istanbul, Türkiye

18

19 *Corresponding author: cdag@ku.edu.tr

20 #equal contribution

21

22

23 **SUMMARY**

24 Crimean-Congo Hemorrhagic Fever (CCHF) is a severe tick-borne viral disease with high
25 mortality rates and significant public health implications. Despite its global prevalence, the
26 mechanisms underlying its pathogenesis remain poorly understood, and effective diagnostic and
27 therapeutic tools are limited. Metabolomics, as a powerful tool for exploring host-pathogen
28 interactions, offers a promising avenue for identifying biomarkers and elucidating disease
29 mechanisms. In this study, we investigated the metabolic alterations in CCHF patients using non-
30 targeted metabolomics to enhance understanding of disease pathogenesis, improve diagnostic
31 capabilities, and identify potential therapeutic targets. A nationwide analysis was conducted on
32 the blood serum of 29 CCHF patients and 10 healthy controls, employing Nuclear Magnetic
33 Resonance (NMR) spectroscopy. Serum samples were collected over four consecutive days, and
34 metabolic profiling was performed using Partial Least Squares Discriminant Analysis (PLS-DA)
35 and Variable Importance in Projection (VIP) scoring to identify key metabolic pathways and
36 compounds. Significant disruptions in metabolic pathways were observed in CCHF patients,
37 particularly in purine and pyrimidine metabolism, the TCA cycle, and redox-related processes.
38 Elevated levels of metabolites such as S-adenosyl homocysteine (SAH), guanosine triphosphate
39 (GTP), inosine monophosphate (IMP), adenosine monophosphate (AMP), carnosine, 2'-
40 deoxyuridine, nicotinamide adenine dinucleotide phosphate (NADP+), and maleate were
41 identified. These metabolites demonstrated potential as biomarkers for disease severity and
42 progression, with distinct metabolic profiles observed between moderate and severe cases. This
43 study provides the first comprehensive metabolomic analysis of CCHF, highlighting critical
44 metabolic pathways disrupted during infection. The findings underscore the utility of NMR-
45 based metabolomics for identifying biomarkers that facilitate early diagnosis, prognosis, and

46 therapeutic development. These results pave the way for future research to validate the identified
47 biomarkers and explore targeted treatment strategies to improve patient outcomes in this severe
48 viral infection.

49 **1. Introduction**

50 Crimean-Congo Hemorrhagic Fever (CCHF) is a severe viral infection with substantial
51 implications for public health in a wide range of countries in Asia, Africa, Southern Europe and
52 the Middle East. CCHF is caused by CCHF virus (CCHFV) belonging to the genus of
53 Orthonairovirus, and the family of Nairoviridae being one of deadliest viruses of its kind with
54 reported mortality rate of 3-30% (1). CCHFV is transmitted to humans through tick bites of
55 infected ticks, contact with blood or tissues of infected livestock, or contact with infected
56 patients (2). The exact course of pathogenesis of CCHF is not clearly known however it is
57 divided into four phases: incubation, pre-haemorrhagic, haemorrhagic and convalescence [2].
58 CCHF is classified as a severe hemorrhagic fever with a short incubation period of 1-3 days
59 although longer incubation periods have been documented [3]. The onset of infection is often
60 sudden and includes symptoms, fever, diarrhea, vomiting, nausea, myalgia, back and abdominal
61 pain followed by an hemorrhagic phase where severe bruises, uncontrollable bleeding at the
62 body orifices are observed and in severe cases, deterioration of kidneys, liver and lungs [4].
63 Deaths associated with the infection mostly occur between 5-14 days from the start of the
64 viremic phase [5]. In terms of treatment, early hospitalizations and early administration of
65 therapeutics are shown to reduce both severity and mortality of CCHF [6]. Hence, lack of early
66 detection of CCHF is one of the leading factors causing the particular high mortality rate of
67 CCHF.

68 There are several challenges of diagnosing CCHF infection particularly before the hemorrhagic
69 phase of the infection and patients who are not suspected of being bitten by infected ticks or
70 contacted with infected livestock. CCHF is comparatively uncommon in specific regions, which
71 may lead healthcare providers to initially overlook it as a potential diagnosis. Likewise, there are
72 documented cases of difficulties diagnosing CCHF, both because of the latter but also the
73 absence of a universally applicable diagnostic kit for surveillance and diagnosis of all CCHFV
74 strains [7]. Standard blood tests such as hemogram, biochemical analysis and physical
75 examination at the beginning of hospitalization is applied on all patients who are suspected to be
76 infected with CCHF although the results are often relevant for short term prognostic factors as
77 biochemical values change often quickly. For more comprehensive and standard diagnostic
78 methods, viral antigen and nucleic acid amplification tests are employed [8]. The initial
79 symptoms of CCHF, such as fever, headache, and muscle aches, are rather non-specific hence
80 diagnosing CCHF early by differential diagnosis can be difficult [5]. However biomarkers,
81 essentially biomolecules, may provide a measure of specific diseases or their stages due to their
82 varying concentrations. Bio markers are instrumental in diagnosing and monitoring the
83 progression of viral infections. The associated changes in their levels, often indicative of the
84 disease, are typically attributed to the host's immune reaction and the disturbance of key
85 biochemical routes in reaction to the infectious process. In this sense, omics studies and
86 biomarkers could be used for both analysis and diagnosis of CCHF and for characterizing better
87 treatment strategies of hospitalized patients swiftly is crucial to pinpoint optimal treatment
88 strategies for treating CCHF [9].

89 So far there is only one omics study which investigates host-viral response and pathogenesis of
90 CCHF utilizing transcriptomics and proteomics methods [10]. Led by this gap in the literature,

91 we conducted a nationwide analysis of metabolomes of patients hospitalized due to CCHF.
92 Turkey has over 10,000 cases of CCHF with an average fatality rate of 5%, making it a critical
93 public health concern affecting people living in rural areas as ticks are widespread in these
94 regions [11]. In our present investigation, we employed Nuclear Magnetic Resonance (NMR)
95 spectroscopy exploratory metabolomics to investigate the overall temporal variations in plasma
96 metabolites during a seasonal outbreak of CCHF infection. We employed PLS-DA statistical
97 analysis of the blood serum metabolome of CCHF patients and categorized certain metabolomes
98 linked to metabolic dysregulation caused by CCHF. Preliminary results from our study suggest
99 that specific metabolic markers can be identified in the serum of CCHF patients pointing to
100 metabolic dysregulation, which may allow for earlier diagnosis and more targeted treatment
101 strategies. Additionally, being the first study to categorize alterations of patient metabolome
102 during CCHF viremic phase may be valuable for efforts to develop therapeutics or targeted
103 treatment strategies to reduce the severity and high mortality rate of CCHF.

104 **2. Materials and methods**

105 **Monitoring of CCHF diagnosed patients and collection of the samples from the patients:**

106 Patients who were diagnosed with CCHF were selected from Çorum Hitit University Hospital.
107 The first sample collection was conducted in April 2022, and blood samples were collected daily
108 using Ethylenediaminetetraacetic acid (EDTA) tubes. In current metabolomics studies, opinions
109 regarding the appropriate determination of sample size can considerably vary. However,
110 numerous statistical analyses have underscored that a substantial sample size, for achieving
111 meaningful results, around 30 samples [12]. In this study, serum specimens were procured from
112 29 patients (n=29) diagnosed with CCHFV infection, as well as from 10 healthy control group.
113 CCHF patients also admitted to the hospital with an infection diagnosis were subclassified into

114 two categories based on their blood test values and symptoms: moderate (n=24) and severe
115 (n=5). Four blood serum samples from patients each consecutive day (n=116 samples) and a
116 single sample from the control group (n=10 samples) was taken. These blood samples were then
117 subjected to centrifugation for 5 minutes at 3000g to separate the sample into plasma, white
118 blood cell, and red blood cell phases. The plasma phase was extracted and subjected to
119 metabolite extraction using multiple approaches: single methanol extraction, triple alcohol
120 extraction, Methanol-chloroform, Acetone, Acetonitrile, and Ultrafiltration. Cold methanol-
121 chloroform was chosen as the most effective extraction and used for extraction of all samples.
122 Only the polar metabolites in the plasma were investigated, while proteins and apolar compounds
123 were removed from the plasma samples. Overall in this study, we utilized a rigorous approach to
124 sample collection, preparation, and analysis to investigate polar metabolites in the plasma of
125 CCHF patients [13].

126 **Ethical Statement:** The study was approved by Koç University Committee on Human Research
127 (01.12.2021/ 2021.436.IRB2.079) and all the procedures performed in this study involving
128 human participants were in accordance with the ethical standards of the institutional research
129 committee ethical standards. A written informed consent was obtained from all patients.

130 **NMR sample preparation:** 4 mL ice-cold methanol-chloroform (1:1) mixture was added to 2
131 mL serum for methanol-chloroform extraction. The mixture was vortexed for 30 seconds and
132 incubated for 10 minutes on ice. After incubation the mixture was centrifuged at 4500g at 4°C
133 for 30 minutes. The methanol phase was collected and dried using a vacuum concentrator. The
134 dried samples were dissolved in 550 uL D₂O based NMR sample solution (50 mM PBS (pH 7.4),
135 20mM NaCl, 1 mM DSS) for standardized sample preparation.

136 **NMR data collection, processing and statistical analysis:** 500 MHz Bruker Ascend magnet
137 with BBO paired resonance probe and Avance NEO console was used for NMR data collection.
138 1D NOESY-presat (noesygppr1d) pulse sequence was used for data collection. Each NMR data
139 spectrum is composed of 4K screening and 32K complex data points. Spectrum widths were set
140 to 9615.4 Hz. Bruker Topspin 4.2.0 software was used for NMR data processing. Data was
141 divided into 0.02 ppm data packages along with their normalization coefficients. The dataset,
142 which comprises data packets with a resolution of 0.02 ppm, was analyzed using the
143 MetaboAnalyst 5.0 online metabolomics statistical analysis software. Henceforth the data will
144 be referred to as (Bin.x.xx [ppm]) data packets and the day of when sample was taken. All data
145 points were normalized using the average centering normalization method. Following this
146 normalization, the dataset underwent statistical analysis using Partial Least Squares Discriminant
147 Analysis (PLS-DA). PLS-DA is a classification and discrimination technique based on the
148 Partial Least Squares (PLS) regression method. This method is widely utilized to determine the
149 differences between classes, particularly in high-dimensional and multivariate datasets. PLS-DA
150 is a commonly employed method in analyzing complex biological systems, such as
151 metabolomics studies. The VIP Projection variable importance score plot is a graph that is
152 utilized to assess the outcomes of PLS-DA and determine the most significant variables in the
153 analysis. VIP scores quantify the importance of each variable (e.g., metabolites) in classification
154 and aid in identifying the most critical features. VIP scores are computed based on the
155 contribution of each variable to the components (latent variables) in the PLS-DA model. The
156 values begin at 1, and higher VIP scores indicate that the variable is more important for
157 classification. Variables with VIP scores greater than 1 are generally deemed significant,
158 although this threshold may vary in practice. The VIP score plot displays the VIP scores of the

159 variables on the vertical axis, while the variables themselves or their indices are shown on the
160 horizontal axis. This graph facilitates the identification of important variables visually and helps
161 focus on the variables that require prioritization in the analysis. In the VIP score graph, the peaks
162 at the relevant ppm values that make up the data packages (Bin.x.xx) have been examined in
163 more detail and the metabolites to which they belong have been identified. For this operation,
164 NMR spectra have been reopened, and the metabolites to which the peak in the relevant ppm
165 region belongs have been determined using the Chenomx software. It is thought that some peaks
166 might belong to metabolites not found in the database, and the molecules these peaks belong to
167 have not been identified. Further investigation and characterization may be required to fully
168 understand these unidentified peaks and their role in the overall metabolic profile, ensuring that
169 the final analysis provides an accurate reflection of the biological system under investigation.

170 **Metabolomic pathway visualization:** All metabolic pathways visualized using Metastate
171 software Version BETA (<https://metastate.bio>) (Metastate Bio Inc.). Metastate algorithm
172 employs the Kyoto Encyclopedia of Genes and Genomes (KEGG) database as its foundational
173 input source. Software systematically retrieves details pertaining to biological pathways,
174 chemical compounds, and molecular reactions of interest. Software curates and assembles a
175 dynamic graphical representation of the data.

176 **3. Results**

177 In this study, 29 patients diagnosed with Crimean-Congo Hemorrhagic Fever (CCHF) and 10
178 healthy individuals serving as control subjects were included. The control group had a mean age
179 of 50.1 years (range: 40–64 years), while the CCHF patient group had a slightly higher mean age
180 of 50.5 years, with a wider age range of 22–77 years. A total of 126 blood samples were

181 collected for analysis. Serum samples were prepared using methanol extraction, followed by
182 Nuclear Magnetic Resonance (NMR) spectroscopy. The metabolite profiles obtained were
183 subjected to comprehensive statistical analysis. This analysis incorporated data from all collected
184 samples over four consecutive days and categorized them into moderate, severe, and control
185 groups for comparative evaluation. Detailed procedures are described in the Materials and
186 Methods section.

187 Partial Least Squares Discriminant Analysis (PLS-DA) was employed to develop a model
188 incorporating the primary components (latent variables) of the dataset. The model focused on the
189 first five components, which were pivotal for data classification and accounted for most of the
190 dataset's variance. The corresponding score plots, presented as two-dimensional graphs, illustrate
191 the pairwise comparisons of these components (Figure 1a).

192 The PLS-DA score plot (Figure 1b) clearly differentiates between healthy and diseased
193 individuals. PLS-DA, well-suited for handling high-dimensional data, effectively identifies the
194 key variables responsible for distinguishing health states. This approach revealed a distinct
195 separation based on variations and correlations within the biomarker data. To further explore the
196 critical contributors to this separation, the Variable Importance in Projection (VIP) scores were
197 analyzed. The PLS-DA VIP score plot (Figure 1c) highlights the variables with the most
198 significant influence on the discrimination process, with the top 15 variables identified. VIP
199 scores provide insights into the relevance of each variable, aiding in the identification of
200 biomarkers that significantly differ between healthy and diseased states.

201 Figure 1c demonstrates that some data buckets exhibit lower concentration values (indicated in
202 blue) in the control group, which progressively increase over time. Furthermore, the identified

203 compounds displayed a marked increase in concentration, as corroborated by enhanced signals
204 from their respective data buckets (Figure 1d).

205 Statistical analysis was performed across three distinct groups, incorporating samples collected
206 over four days from both patient groups. While patient samples were successfully distinguished
207 from the control group, no significant differences were observed between the moderate and
208 severe disease groups. Key metabolites found to be elevated in the patient groups compared to
209 controls included SAH, GTP, carnosine, maleate, 2-deoxyuridine, IMP, AMP, and NADP+.

210 As a secondary approach to data analysis, metabolite profiles were evaluated using samples
211 collected on days 1 and 2 of hospitalization, representing the early stages of infection. Patients
212 were categorized into severe and moderate groups based on clinical severity, while blood
213 samples from healthy individuals were used as the control group for statistical comparisons
214 (Figure 2). This focused analysis aimed to investigate metabolite changes during the initial phase
215 of the disease. In addition to compounds identified in the initial analysis, novel metabolites with
216 significant increases on days 1 and 2 were detected, suggesting their potential involvement in the
217 pathogenesis of Crimean-Congo Hemorrhagic Fever (CCHF).

218 A comprehensive metabolomic analysis of blood serum from CCHF patients revealed distinct
219 metabolite patterns corresponding to infection severity. Partial Least Squares Discriminant
220 Analysis (PLS-DA) score plots and Variable Importance in Projection (VIP) scores (Figure 3)
221 highlighted notable differences in metabolite profiles between severe and moderate cases. In
222 severe CCHF infections, metabolites such as AMP, IMP, and NAAD were significantly elevated
223 in the serum, whereas these compounds were less prominent in samples from patients with

224 moderate infection. Conversely, GTP was markedly increased in the moderate infection group
225 but was not significantly detected in the severe group.

226 Overall, these findings highlight substantial metabolic differences between moderate and severe
227 CCHF infections, pointing to critical pathways potentially involved in CCHF pathogenesis.
228 These results underscore the importance of early-stage metabolite profiling to enhance our
229 understanding of disease mechanisms and identify potential biomarkers for severity
230 stratification.

231 **4. Discussion**

232
233 In this study, we present the first non-targeted metabolomics analysis of Crimean-Congo
234 Hemorrhagic Fever (CCHF) to enhance the understanding of its pathogenesis, improve
235 diagnostic capabilities, and aid in the development of potential therapeutic interventions. Using
236 Nuclear Magnetic Resonance (NMR) spectroscopy, we identified significant increases in key
237 metabolites, including S-adenosyl homocysteine (SAH), guanosine triphosphate (GTP),
238 carnosine, maleate, 2'-deoxyuridine (2'-dU), inosine monophosphate (IMP), adenosine
239 monophosphate (AMP), and nicotinamide adenine dinucleotide phosphate (NADP+), in the
240 blood serum of CCHF patients. These findings suggest that these metabolites may play critical
241 roles in the pathogenesis of CCHF and serve as important biomarkers for early detection and
242 monitoring of disease progression.

243 Metabolomics has emerged as a powerful tool for studying host-pathogen interactions by
244 revealing metabolic alterations induced by viral infections. To date, only one prior omics study
245 utilizing mass spectrometry (MS) has investigated the interaction between the host and CCHF

246 virus (CCHFV). Both NMR and MS are widely used in metabolomics, with each method
247 offering distinct advantages depending on the research objectives. NMR spectroscopy is
248 particularly suitable for non-targeted metabolomics due to its superior reproducibility, minimal
249 sample preparation, and ability to analyze complex biofluids. It also provides consistent spectra
250 across different instruments and laboratories, making it highly reliable for diagnostic and
251 prognostic studies. On the other hand, MS offers higher sensitivity and is often preferred for
252 targeted metabolomics studies.

253 The utility of NMR metabolomics has been demonstrated in the analysis of host metabolic
254 changes induced by various viral infections, including HIV, dengue virus (DENV), and
255 chikungunya virus. Moreover, metabolomics approaches have been successfully applied to study
256 other viral hemorrhagic fevers, such as Ebola, Marburg, and dengue, yielding promising results
257 for early diagnosis and prognosis prediction. Similarly, our findings underscore the potential of
258 NMR metabolomics in elucidating the complex metabolic interactions between CCHFV and its
259 host. The observed metabolic changes in CCHF patients offer new insights into the mechanisms
260 of disease pathogenesis and highlight potential pathways for targeted therapeutic interventions.

261 By focusing on metabolite profiles in CCHF, this study demonstrates the value of NMR-based
262 metabolomics in addressing the gaps in knowledge surrounding this severe disease. Our findings
263 not only advance the understanding of CCHF pathogenesis but also provide a foundation for
264 further research aimed at identifying effective biomarkers and therapeutic targets. These results
265 emphasize the critical role of metabolomics in uncovering host-pathogen dynamics and
266 improving clinical outcomes in viral infections.

267 Among the notable metabolites detected, S-adenosyl homocysteine (SAH) emerged as a
268 significant intermediate in the metabolic pathways of CCHF patients. SAH, a precursor to
269 homocysteine and adenosine, serves as the substrate for the enzyme SAH hydrolase, a critical
270 component of the S-adenosylmethionine (SAM/AdoMet) regeneration cycle (Figure 4a).
271 Elevated SAH levels were observed in CCHF patients early during hospitalization, underscoring
272 its potential relevance in the disease's pathogenesis. This observation aligns with findings from a
273 genomic study linking Methylenetetrahydrofolate reductase (MTHFR) polymorphisms to a
274 predisposition for milder forms of CCHF [18]. Since MTHFR plays a central role in folate
275 metabolism and methylation processes, these results suggest that disruptions in methylation
276 pathways during the viremic phase could serve as prognostic indicators for CCHF severity.

277 SAM is a key methyl donor in various cellular methylation reactions, including those involved in
278 5' RNA capping, a process critical for viral replication and transcription [19]. Evidence from
279 other viral families, such as flaviviruses [20], and Ebola, whose L protein exhibits
280 methyltransferase activity, indicates that methylation mechanisms can influence RNA cap
281 structure and internal adenosine-2'-O-methylation [21]. These parallels highlight the potential
282 importance of methylation pathways in CCHF pathogenesis. The additional complexity of RNA
283 methylation in some viral families suggests that SAM-related domains within viral replication
284 complexes could represent promising therapeutic targets.

285 Our findings emphasize the need for further research into SAM-related pathways to unravel their
286 implications for viral replication and host-pathogen interactions in CCHF. These pathways not
287 only provide insight into disease mechanisms but also present opportunities for the development
288 of targeted therapeutic interventions, particularly those aimed at disrupting key methylation
289 processes critical for viral survival.

290 GTP, AMP, and inosine monophosphate (IMP) are key nucleotides involved in purine
291 metabolism, essential for energy production and nucleic acid synthesis (Figure 4b). Elevated
292 levels of GTP and IMP are well-documented indicators of viral infections, particularly among
293 viruses in the *Orthornavirae* kingdom. In the context of CCHF, the increase in these purine
294 metabolites aligns with the known mechanism of action of broad-spectrum antivirals like
295 Ribavirin. As a nucleotide analog, Ribavirin targets the substrate-binding site of the IMPDH
296 enzyme, thereby reducing RNA synthesis in infected cells by downregulating GTP synthesis
297 [22]. Monitoring these metabolites could provide valuable insights into the efficacy of antiviral
298 treatments. Additionally, quantifying shifts in GTP and IMP concentrations offers a potential
299 strategy to optimize therapeutic interventions in clinical trials, enhancing the effectiveness of
300 antiviral agents targeting purine metabolism [23].

301 Carnosine (β -alanyl-L-histidine) (Figure 4c), a dipeptide with antioxidant, anti-glycation, and
302 anti-inflammatory properties, was also significantly elevated in CCHF patients. Predominantly
303 found in skeletal muscle and the brain, increased carnosine levels may reflect a compensatory
304 response to oxidative stress, infection-induced cell death, or muscle mass reduction due to
305 hospitalization. Carnosine has demonstrated antiviral potential against Zika, dengue, and SARS-
306 CoV-2, reducing viral replication and alleviating symptoms. While its therapeutic utility against
307 CCHF remains to be established, these findings highlight the need for further investigation into
308 its potential as a treatment option.

309 2'-Deoxyuridine (2'-dU), an intermediate in thymidylate synthesis (Figure 4d), also showed
310 significant elevation in CCHF patients. This metabolite, a precursor for DNA synthesis, plays a
311 role in antiviral therapies, such as Edoxudine, which target DNA viruses [24–26]. Variants of 2'-
312 dU, such as BVDU, have shown efficacy against Herpes simplex virus type 1 (HSV-1) and

313 varicella-zoster virus (VZV) [27]. While 2'-dU is typically associated with DNA virus activity,
314 its elevated levels in CCHF patients may suggest broader disruptions in pyrimidine metabolism,
315 potentially linked to the metabolic dysregulation observed in this study.

316 Nicotinamide adenine dinucleotide phosphate (NADP⁺) serves as a critical cofactor in enzymatic
317 reactions, primarily within the pentose phosphate pathway, where it supports fatty acid synthesis
318 and the regeneration of reduced glutathione. Its role in redox reactions also underscores its
319 importance in the antioxidant defense system. Elevated NADP⁺ levels in CCHF patients could
320 reflect increased metabolic activity related to energy production and nucleotide synthesis. This
321 hypothesis is further supported by the observed overlap in the elevations of NADP⁺, GTP, IMP,
322 and AMP, indicating a coordinated upregulation of energy metabolism pathways. The significant
323 increase in these metabolites in severe cases (Figure 3) underscores their potential relevance in
324 disease progression and severity.

325 Maleate (cis-butenedioic acid), a dicarboxylic acid and trans-isomer of fumaric acid, plays a role
326 in nicotinate and nicotinamide metabolism [29]. Elevated maleate levels in CCHF patients
327 suggest underlying metabolic disruptions. Previous studies have demonstrated that maleate can
328 inhibit the tricarboxylic acid (TCA) cycle, lower ATP levels, and impair enzymatic activity,
329 leading to systemic metabolic imbalances. These findings warrant further investigation into the
330 potential implications of maleate in the pathophysiology of CCHF [30].

331 In summary, these metabolomic findings reveal significant disruptions in purine, pyrimidine, and
332 energy metabolism pathways in CCHF patients. Metabolites such as GTP, IMP, AMP, carnosine,
333 2'-dU, NADP⁺, and maleate provide valuable insights into the pathogenesis of the disease and
334 highlight potential biomarkers for disease progression and therapeutic targets.

335

336

337

338 **Conclusion**

339 In this study, we conducted a nationwide analysis of blood serum metabolites from patients
340 hospitalized due to Crimean-Congo Hemorrhagic Fever (CCHF), employing Nuclear Magnetic
341 Resonance (NMR) spectroscopy as a novel approach to investigate host-pathogen interactions
342 and the pathogenesis of CCHFV. Our findings revealed significant alterations in several key
343 metabolites, including S-adenosyl homocysteine (SAH), guanosine triphosphate (GTP), inosine
344 monophosphate (IMP), adenosine monophosphate (AMP), 2'-deoxyuridine (2'-dU), nicotinamide
345 adenine dinucleotide phosphate (NADP⁺), carnosine, and maleate. Notable changes were
346 observed in pathways related to the TCA cycle, nucleic acid synthesis, and redox-associated
347 coenzymes, highlighting the systemic metabolic impact of CCHFV infection.

348 The elevation of metabolites such as SAH underscores the potential impact of methylation
349 processes on CCHF pathogenesis and prognosis, linking viral replication to host epigenetic
350 regulation. Similarly, the observed disruptions in purine metabolism, particularly the increased
351 levels of GTP and IMP, suggest potential therapeutic implications, as these pathways are
352 targeted by antiviral agents like Ribavirin. The role of other metabolites, such as carnosine and
353 maleate, indicates a systemic response to oxidative stress and cellular damage, providing further
354 insight into the host's metabolic adaptation during infection.

355 Our findings align with prior metabolomics studies on other viral hemorrhagic fevers and
356 highlight the utility of NMR-based metabolomics for uncovering biomarkers that may facilitate
357 early diagnosis, prognosis prediction, and therapeutic development. The distinct metabolic
358 profiles observed between moderate and severe CCHF cases further emphasize the relevance of
359 these biomarkers in stratifying disease severity and monitoring treatment efficacy.

360 This study paves the way for future investigations to validate these biomarkers in larger cohorts
361 and explore the therapeutic potential of targeting the identified pathways. By advancing the
362 understanding of CCHF pathogenesis, our results contribute to the development of more
363 effective diagnostic and therapeutic strategies, ultimately improving patient outcomes in this
364 severe viral infection.

365 **Author Contributions**

366 **Çağdaş Dağ:** Conceptualization, Methodology, Supervision, Funding acquisition, Writing-
367 Reviewing and Editing, Writing-Original draft preparation **Kerem Kahraman:** Investigation,
368 Formal analysis, Visualization, Writing-Reviewing and Editing **Oktay Göcenler:** Investigation,
369 Formal analysis, Writing-Original Draft, Visualization **Derya Yapar:** Investigation **Yaren**
370 **Kahraman:** Investigation, Formal analysis **Cengizhan Büyükdag:** Formal analysis, Writing-
371 Original Draft **Gülen Esken:** Methodology, Investigation **Serena Ozabrahamyan:**
372 Methodology, Investigation **Tayfun Barlas:** Investigation **Yüksel Karadağ:** Investigation **Aysel**
373 **Kocagül Çelikbaş:** Investigation **Fusun Can:** Supervision, Investigation **Nurcan Baykam:**
374 Supervision, Investigation **Mert Kuşkucu:** Supervision, Writing-Reviewing and Editing **Önder**
375 **Ergönül:** Supervision, Funding acquisition, Conceptualization, Methodology

376 ACKNOWLEDGMENT

377 CD acknowledges support from TU□BI□TAK (Project No: 221S353). The authors
378 acknowledge the use of the services and facilities of n²STAR-Koç University Nanofabrication
379 and Nanocharacterization Center for Scientific and Technological Advanced Research. The
380 authors gratefully acknowledge use of the services and facilities of the Koc□ University Is Bank
381 Infectious Disease Center (KUIS-CID). We are also immensely grateful to Firat Kahya, Boran
382 Saruhan and Oğuzcan Ünver for constructive feedback and for their comments.

383 References

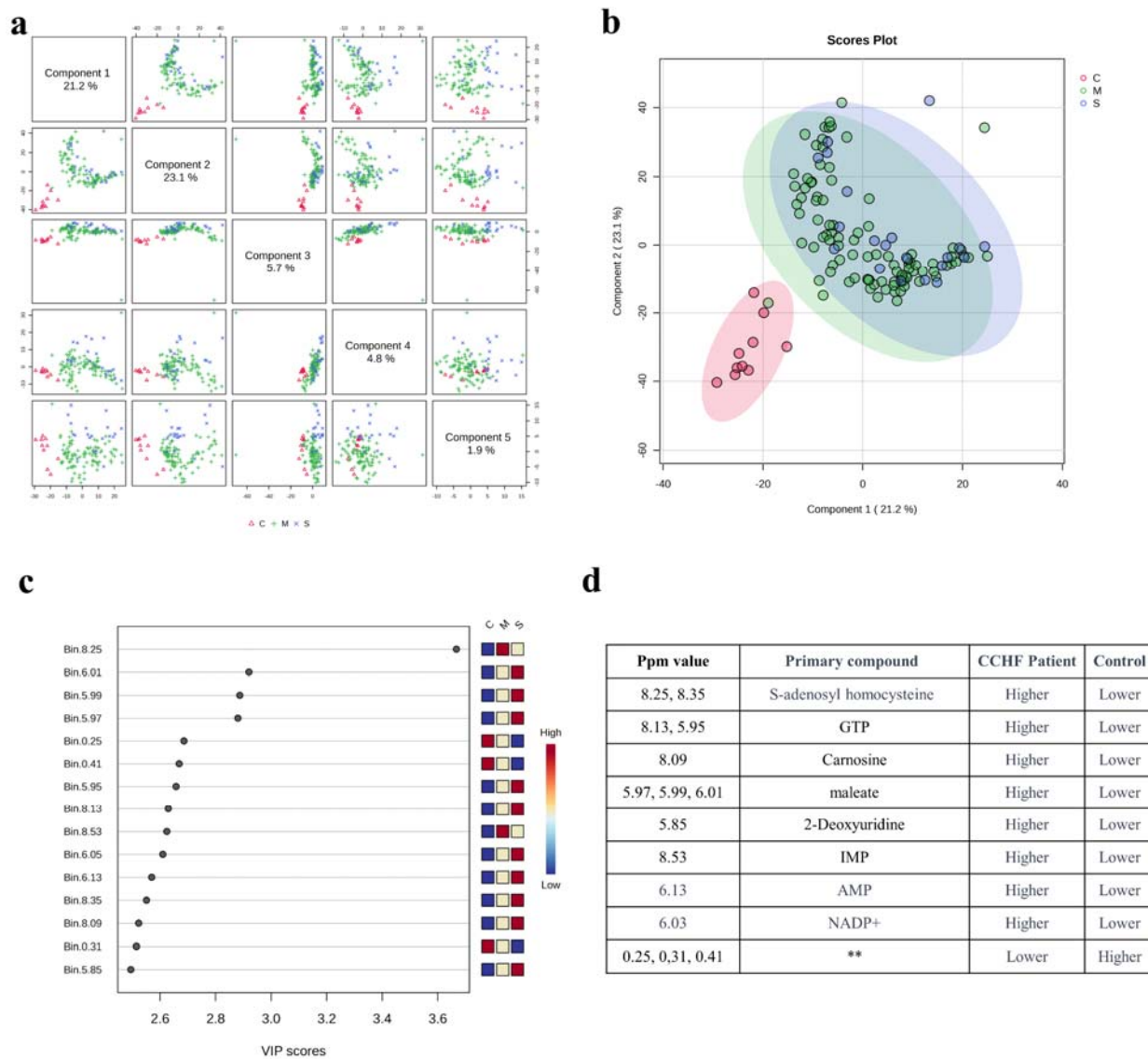
- 384 [1] Belhadi, D., Baied, M. E., Mulier, G., Malvy, D., Mentré, F., & Laouénan, C. (2022). The
385 number of cases, mortality and treatments of viral hemorrhagic fevers: A systematic review.
386 PLOS Neglected Tropical Diseases, 16(10), e0010889.
387 <https://doi.org/10.1371/journal.pntd.0010889>
- 388 [2] Hoogstraal H. (1979). The epidemiology of tick-borne Crimean-Congo hemorrhagic fever in
389 Asia, Europe, and Africa. *Journal of medical entomology*, 15(4), 307–417.
390 <https://doi.org/10.1093/jmedent/15.4.307>
- 391 [3] Whitehouse, C. A. (2004). Crimean-Congo hemorrhagic fever. *Antiviral Research*, 64(3),
392 145–160. <https://doi.org/10.1016/j.antiviral.2004.08.001>
- 393 [4] Elaldi, N., Bodur, H., Ascioğlu, S., Celikbas, A. K., Özkurt, Z., Vahaboglu, H.,
394 Leblebicioglu, H., Yilmaz, N., Engin, A., Şencan, M., Aydin, K., Dokmetas, I., Çevik, M. A.,
395 Dokuzoğuz, B., Tasyaran, M. A., Öztürk, R., Bakir, M., & Uzun, R. (2009). Efficacy of oral
396 ribavirin treatment in Crimean-Congo haemorrhagic fever: A quasi-experimental study from
397 Turkey. *Journal of Infection*, 58(3), 238–244. <https://doi.org/10.1016/j.jinf.2009.01.014>
- 398 [5] Swanepoel, R., Gill, D. E., Shepherd, A. J., Leman, P. A., Mynhardt, J. H., & Harvey, S.
399 (1989). The clinical pathology of Crimean-Congo hemorrhagic fever. *Reviews of infectious*
400 *diseases*, 11 Suppl 4, S794–S800. https://doi.org/10.1093/clinids/11.supplement_4.s794
- 401 [6] Ergonul O. (2008). Treatment of Crimean-Congo hemorrhagic fever. *Antiviral research*,
402 78(1), 125–131. <https://doi.org/10.1016/j.antiviral.2007.11.002>
- 403 [7] Almayahi, Z. K., Kindi, H. A., Jabri, I. H. S. H. A., Shaqsi, N. H. K. A., Hattali, N. A.,
404 Hattali, A. A., Quyoodhi, B. A., & Dhuhli, K. A. (2022). Challenges in Diagnosis of Crimean-
405 Congo Hemorrhagic Fever. *Infectious Diseases in Clinical Practice*, 30(2).
406 <https://doi.org/10.1097/ipc.0000000000001108>

- 407 [8] Raabe V. N. (2020). Diagnostic Testing for Crimean-Congo Hemorrhagic Fever. *Journal of*
408 *clinical microbiology*, 58(4), e01580-19. <https://doi.org/10.1128/JCM.01580-19>
- 409 [9] Mayne, E. S., George, J. A., & Louw, S. (2023). Assessing Biomarkers in Viral Infection.
410 *Advances in experimental medicine and biology*, 1412, 159–173. <https://doi.org/10.1007/978-3->
411 031-28012-2_8
- 412 [10] Neogi, U., Elaldi, N., Appelberg, S., Ambikan, A. T., Kennedy, E. V., Dowall, S. D., Bagci,
413 B., Gupta, S., Murillo, J. R., Akusjärvi, S. S., Monteil, V., Marko-Varga, G., Benfeitas, R.,
414 Banerjea, A. C., Weber, F., Hewson, R., & Mirazimi, A. (2022). Multi-omics insights into host-
415 viral response and pathogenesis in Crimean-Congo hemorrhagic fever viruses for novel
416 therapeutic target. *eLife*, 11. <https://doi.org/10.7554/elife.76071>
- 417 [11] Ak, Ç., Ergönül, Ö. & Gönen, M. A prospective prediction tool for understanding Crimean–
418 Congo haemorrhagic fever dynamics in Turkey. *Clin. Microbiol. Infect.* 26, 123-e1 (2020).
- 419 [12] Nyamundanda, G., Gormley, I.C., Fan, Y. et al. MetSizeR: selecting the optimal sample size
420 for metabolomic studies using an analysis based approach. *BMC Bioinformatics* 14, 338 (2013).
421 <https://doi.org/10.1186/1471-2105-14-338>
- 422 [13] Markley, J. L., Brüschweiler, R., Edison, A. S., Eghbalnia, H. R., Powers, R., Raftery, D., &
423 Wishart, D. S. (2017). The future of NMR-based metabolomics. *Current opinion in*
424 *biotechnology*, 43, 34–40. <https://doi.org/10.1016/j.copbio.2016.08.001>
- 425 [14] Emwas, A. M. (2015). The Strengths and Weaknesses of NMR Spectroscopy and Mass
426 Spectrometry with Particular Focus on Metabolomics Research. In *Methods in molecular biology*
427 (pp. 161–193). Springer Science+Business Media. [https://doi.org/10.1007/978-1-4939-2377-](https://doi.org/10.1007/978-1-4939-2377-9_13)
428 9_13
- 429 [15] Munshi, S. U., Rewari, B. B., Bhavesh, N. S., & Jameel, S. (2013). Nuclear magnetic
430 resonance based profiling of biofluids reveals metabolic dysregulation in HIV-infected persons
431 and those on anti-retroviral therapy. *PloS one*, 8(5), e64298.
432 <https://doi.org/10.1371/journal.pone.0064298>
- 433 [16] Shrinet, J., Shastri, J. S., Gaind, R., Bhavesh, N. S., & Sunil, S. (2016). Serum
434 metabolomics analysis of patients with chikungunya and dengue mono/co-infections reveals
435 distinct metabolite signatures in the three disease conditions. *Scientific reports*, 6, 36833.
436 <https://doi.org/10.1038/srep36833>
- 437 [17] Wang, Z., Liang, H., Cao, H., Zhang, B., Li, J., Wang, W., Qin, S., Wang, Y., Xuan, L., Lai,
438 L., & Shui, W. (2019). Efficient ligand discovery from natural herbs by integrating virtual
439 screening, affinity mass spectrometry and targeted metabolomics. *Analyst*, 144(9), 2881–2890.
440 <https://doi.org/10.1039/c8an02482k>
- 441 [18] Karakus, N., Duygu, F., Rustemoglu, A., & Yigit, S. (2022). Methylene-tetrahydrofolate
442 reductase gene C677T and A1298C polymorphisms as a risk factor for Crimean-Congo
443 hemorrhagic fever. *Nucleosides, Nucleotides & Nucleic Acids*, 41(9), 878–890.
444 <https://doi.org/10.1080/15257770.2022.2085296>

- 445 [19] Byszewska, M., Śmietański, M., Purta, E., & Bujnicki, J. M. (2014). RNA
446 methyltransferases involved in 5' cap biosynthesis. *RNA Biology*, 11(12), 1597–1607.
447 <https://doi.org/10.1080/15476286.2015.1004955>
- 448 [20] Brecher, M., Chen, H. S., Liu, B., Banavali, N. K., Jones, S., Zhang, J., Li, Z., Kramer, L.
449 D., & Li, H. (2015b). Novel Broad Spectrum Inhibitors Targeting the Flavivirus
450 Methyltransferase. *PLOS ONE*, 10(6), e0130062. <https://doi.org/10.1371/journal.pone.0130062>
- 451 [21] Valle, C., Martin, B., Ferron, F., Roig-Zamboni, V., Desmyter, A., Debart, F., Canard, B.,
452 Coutard, B., & Decroly, E. (2021). First insights into the structural features of Ebola virus
453 methyltransferase activities. *Nucleic Acids Research*, 49(3), 1737–1748.
454 <https://doi.org/10.1093/nar/gkaa1276>
- 455 [22] Tchesnokov, E. P., Bailey-Elkin, B. A., Mark, B. L., & Götte, M. (2020). Independent
456 inhibition of the polymerase and deubiquitinase activities of the Crimean-Congo Hemorrhagic
457 Fever Virus full-length L-protein. *PLOS Neglected Tropical Diseases*, 14(6), e0008283.
458 <https://doi.org/10.1371/journal.pntd.0008283>
- 459 [23] Robins, R. K., Revankar, G. R., McKernan, P. A., Murray, B. K., Kirsi, J. J., & North, J. A.
460 (1985). The importance of IMP dehydrogenase inhibition in the broad spectrum antiviral activity
461 of ribavirin and selenazofurin. *Advances in Enzyme Regulation*, 24, 29–43.
462 [https://doi.org/10.1016/0065-2571\(85\)90068-8](https://doi.org/10.1016/0065-2571(85)90068-8)
- 463 [24] Rothan, H. A., Abdulrahman, A. Y., Khazali, A. S., Rashid, N. N., Chong, T. T., & Yusof,
464 R. (2019). Carnosine exhibits significant antiviral activity against Dengue and Zika virus.
465 *Journal of Peptide Science*, 25(8). <https://doi.org/10.1002/psc.3196>
- 466 [25] Saadah, L. M., Deiab, G. I. A., Al-Balas, Q., & Basheti, I. A. (2020). Carnosine to Combat
467 Novel Coronavirus (nCoV): Molecular Docking and Modeling to Cocrystallized Host
468 Angiotensin-Converting Enzyme 2 (ACE2) and Viral Spike Protein. *Molecules*, 25(23), 5605.
469 <https://doi.org/10.3390/molecules25235605>
- 470 [26] Chon, J., Stover, P. J., & Field, M. S. (2017). Targeting nuclear thymidylate biosynthesis.
471 *Molecular Aspects of Medicine*, 53, 48–56. <https://doi.org/10.1016/j.mam.2016.11.005>
- 472 [27] De Clercq E. (2005). Potential clinical applications of the CXCR4 antagonist bicyclam
473 AMD3100. *Mini reviews in medicinal chemistry*, 5(9), 805–824.
474 <https://doi.org/10.2174/1389557054867075>
- 475 [28] Yen, Y. C., Kong, L. X., Lee, L., Zhang, Y. Q., Li, F., Cai, B. J., & Gao, S. Y. (1985).
476 Characteristics of Crimean-Congo hemorrhagic fever virus (Xinjiang strain) in China. *The*
477 *American journal of tropical medicine and hygiene*, 34(6), 1179–1182
- 478 [29] National Center for Biotechnology Information (2023). PubChem Compound Summary for
479 CID 444266, Maleic Acid. Retrieved August 15, 2023 from
480 <https://pubchem.ncbi.nlm.nih.gov/compound/Maleic-Acid>

481 [30] Bergeron, M. G., Mayers, P., & Brown, D. T. (1996). Specific effect of maleate on an apical
 482 membrane glycoprotein (gp330) in proximal tubule of rat kidneys. *American Journal of*
 483 *Physiology-renal Physiology*, 271(4), F908–F916.
 484 <https://doi.org/10.1152/ajprenal.1996.271.4.f908>

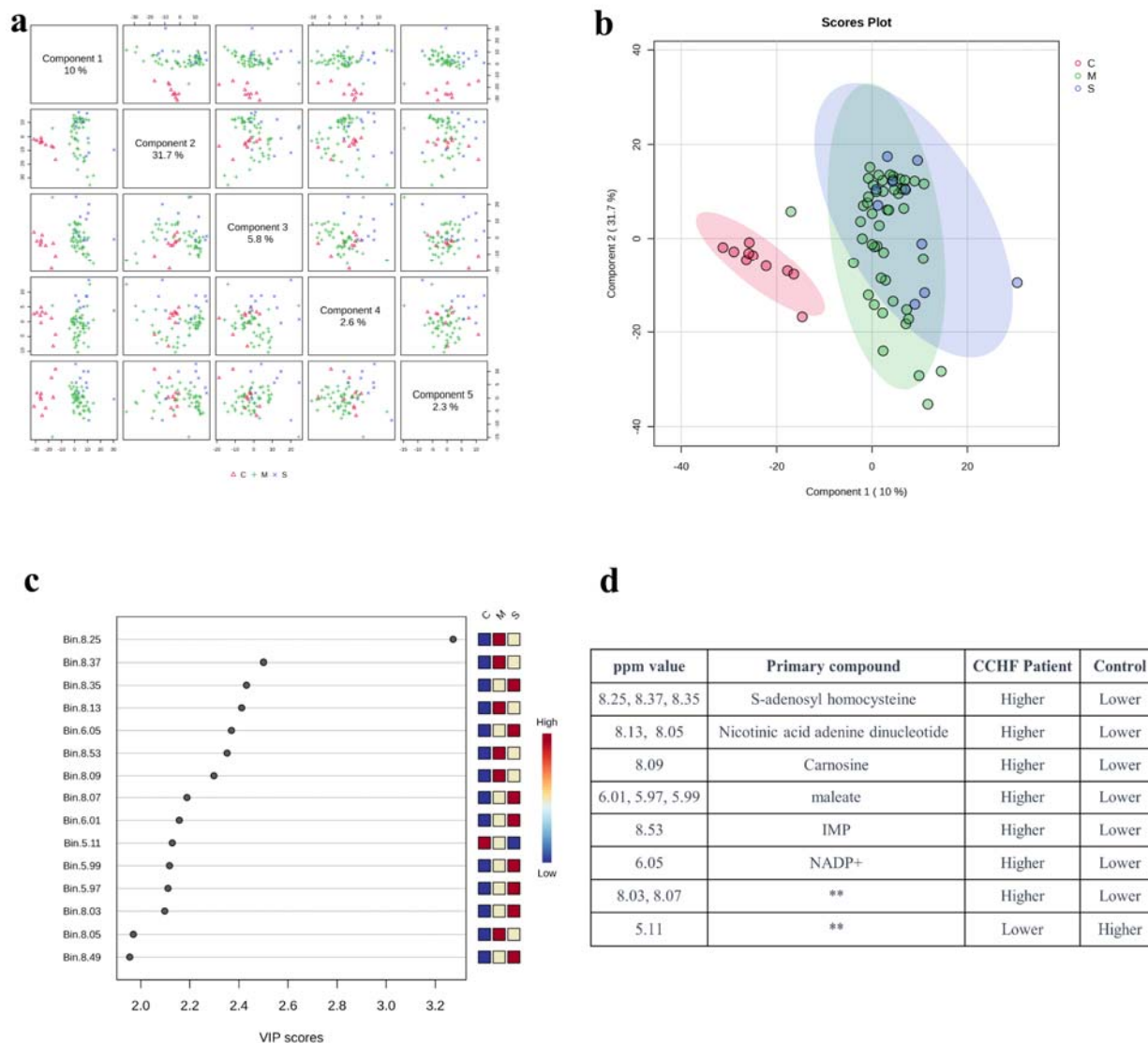
485



486

487 **Figure 1** PLS-DA analysis of patient samples with severe and moderate infection level for four
 488 consecutive days with the control group (S: severe, M: moderate, C: Control) a. Matching score
 489 plots for the first five components of the PLS-DA analysis of all samples. b. partial Least
 490 Squares Discriminant Analysis score plot. c. Variable importance score plot in PLS-DA VIP
 491 Projection. d. corresponding compounds in detected increases on the spectra. Component 1:
 492 accuracy=0.817, (R2=0.246, Q2=0.142), component 2: accuracy=0.833, (R2=0.394, Q2=0.210),

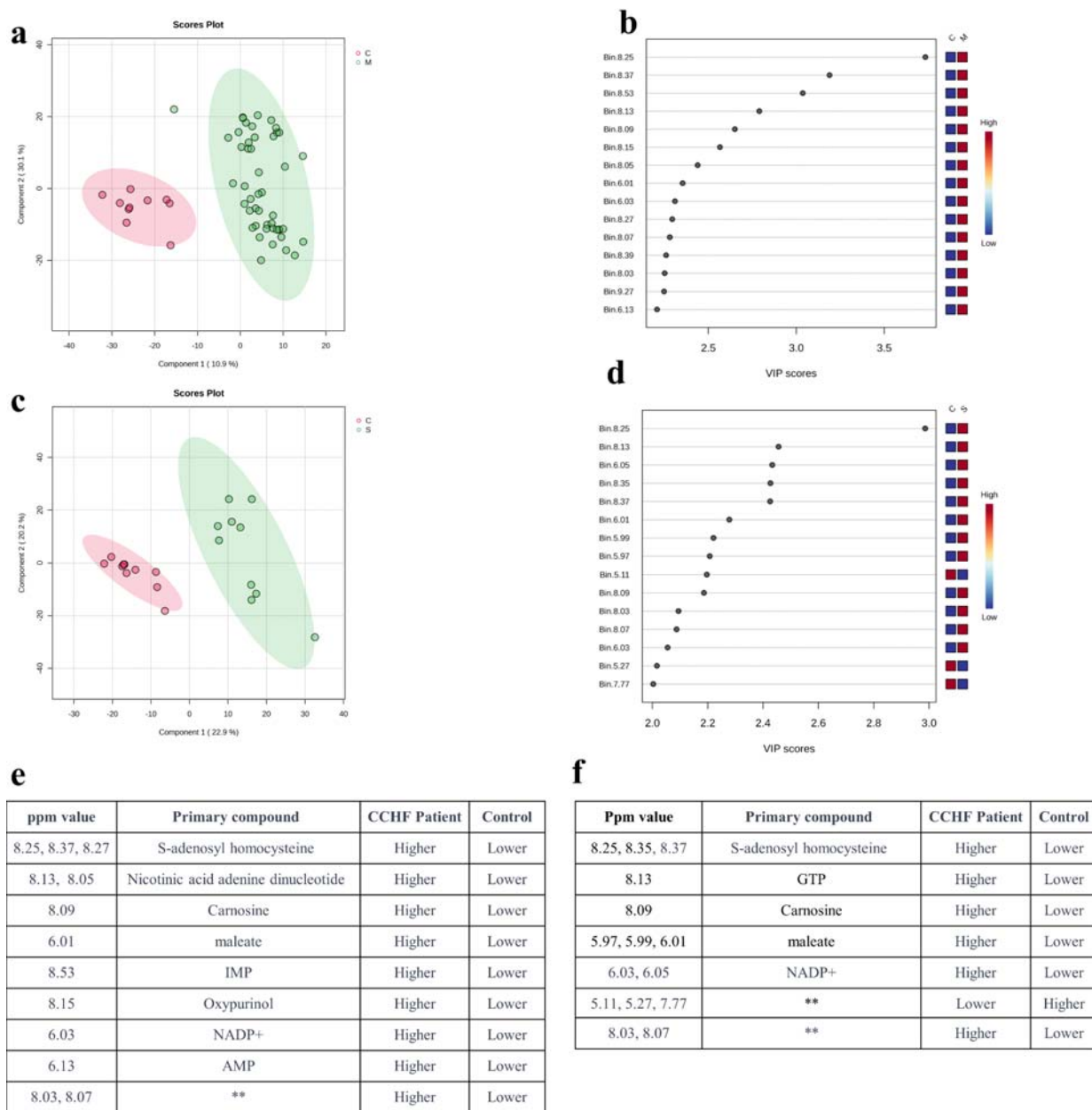
493 component 3: accuracy=0.809, (R2=0.545, Q2=0.225), component 4: accuracy=0.777,
 494 (R2=0.644, Q2=0.250), component 5: accuracy=0.769, (R2=0.782, Q2=0.205)
 495



496

497

498 **Figure 2** PLS-DA analysis of patient samples with severe and moderate infection level for first
 499 two days with the control group matching score plots for the first five components of the PLS-
 500 DA analysis of samples from day 1 and day 2 as labeled mild (M), severe (S) and compared with
 501 the control group (C). b, partial Least Squares Discriminant Analysis score plot. c, Variable
 502 importance score plot in PLS-DA VIP Projection. d, corresponding compounds in detected
 503 increases on the spectra. Component 1: accuracy=0.0837, (R2=0.585, Q2=0.417), component 2:
 504 accuracy=0.821, (R2=0.627, Q2=0.433), component 3: accuracy=0.793, (R2=0.804, Q2=0.352)
 505



506

507 **Figure 3** PLS-DA analysis of patient samples with moderate infection level for first two days
 508 with the control group and PLS-DA analysis of patient samples with severe infection level for
 509 first two days with the control group (S:severe, M: moderate, C:Control) a, partial Least Squares
 510 Discriminant Analysis score plot. Component 1: accuracy=0.983, (R2=0.821, Q2=0.739),
 511 component 2: accuracy=0.983, (R2=0.860, Q2=0.790), component 3: accuracy=0.983,
 512 (R2=0.954, Q2=0.829) b, Variable importance score plot in PLS-DA VIP Projection. c, partial
 513 Least Squares Discriminant Analysis score plot. Component 1: accuracy=0.950, (R2=0.857,
 514 Q2=0.702), component 2: accuracy=1, (R2=0.938, Q2=0.797), component 3: accuracy=1,
 515 (R2=0.982, Q2=0.824) d, Variable importance score plot in PLS-DA VIP Projection. e,
 516 corresponding compounds in detected increases on the spectra. f, corresponding compounds in
 517 detected increases on the spectra.

